

MEASUREMENT AND INTERPRETATION OF VIBRATION RESPONSE OF A CONCRETE PEDESTAL CAST OVER BEDROCK

Y.S. Bhadauria, S.K. Arora and Vijai Kumar
Seismology Section
Bhabha Atomic Research Centre
Trombay, BOMBAY - 400 085

ABSTRACT

In this paper we present vibratory characteristics of a typical concrete pedestal cast over bedrock in a ground floor room of a large laboratory building at our Centre, to mount a sensitive spectrometer on it. Around this pedestal is provided a rectangular channel of small width filled with dry sand as vibration damper. In a seismic experiment, the vibration isolation response (transmissibility) of this pedestal has been measured and interpreted. The transmissibility has been computed from power spectra of artificially generated transient signals produced at the time of the experiment by dropping a small weight on the floor and detected simultaneously by seismic sensors installed at the base as well as at the top of the pedestal. Essentially, the coherence between such pairs of signals has been used to interpret the transmissibility peaks. From the wide band accelerographic data, the pedestal is found to have appreciable transmissibility in the frequency band 90-110 Hz peaking at 102 Hz.

INTRODUCTION

Ambient vibrations pose a serious limitation on the performance of a variety of equipment used for making linear or angular measurements in many areas like Optics, Lasers, Spectroscopy, Semiconductor technology, and so on. Consider, for instance, the task of photographing a highly magnified image of a tiny object through a microscope and camera assembly. The relative position of different components of this system, namely the microscope, the camera, the illuminator and the object determine where exactly on the film plane each point of the image will be photographed. If, during the exposure time, all components of the system remain either stationary or move together so that there is no relative displacement among them, the image will be sharp and clear. On the other hand, if the components of the system move randomly, the image will be blurred.

The relative random motion among different components of the equipment is produced by mainly ambient vibrations. Among various local sources of ambient vibrations, some can be eliminated while seismic effects due to some others can be suppressed in a selected frequency band by employing suitable techniques of vibration isolation.

Vibration isolation or base isolation techniques can broadly be classified into two categories; (i) active vibration isolation techniques and (ii) passive vibration isolation techniques (Hunt, 1979). Active vibration isolators, although very effective for vibration isolation purpose, are very complex and expensive and also require external power for their operation (Hong Su et al., 1990).

A passive vibration isolator, on the other hand, is relatively simple. In its most elementary form such an isolator may be considered as a resilient member (spring) connecting the equipment with the floor through some energy dissipating mechanism (damper). Trenches filled with damping materials like sand or rock around precast

concrete blocks are also commonly used for vibration isolation purpose (see, for example, Crede and Harris, 1976; Lavania and Bandyopadhyay, 1989).

In this paper, some useful practical aspects of vibration isolation are presented alongwith the measured isolation response (transmissibility) of a typical concrete pedestal of cross sectional area 5 ft. x 3 ft. and 4 ft. in height cast on a larger sized (6 ft. x 4 ft. x 4 ft.) concrete footing raised over the bedrock. Designed to set up a sensitive spectrometer on it, this pedestal structure is housed in a room at the ground floor of a large laboratory building at BARC. Around it, a rectangular channel of average width about eight inches (6 inches at bottom and about 10 inches at the floor level) consisting of dry sand is provided to damp ambient vibrations. Figure 1 shows a schematic diagram of the pedestal (Krishnamurthy, 1991).

THEORETICAL ASPECTS OF VIBRATION ISOLATION

A simple vibration isolator modeled conceptually as a single degree of freedom mass-spring-damping system has three main components, namely the total mass of the platform and equipment mounted over it, the spring and the damper. If the spring is composed of material like rubber, cork or sand, damping is automatically built into the spring in the form of internal material damping (Broch, 1972).

The response, $x(t)$, of this structure of total mass M , to floor vibration input having displacement $u(t)$, is given by the solution of the equation (Crede and Harris 1976).

$$M \frac{d^2 x}{dt^2} + C \frac{d(x-u)}{dt} + K(x-u) = 0 \quad (1)$$

where C is the damping coefficient of the material and K is the spring constant, also known as stiffness of the spring.

The general solution in frequency domain (w) of equation (1) is given by :

$$X(w) = H(w) \cdot U(w) \quad (2)$$

where $X(w)$ and $U(w)$ are the Fourier transforms of the time series, $x(t)$ and $u(t)$, corresponding to vibrations on the top and at the base of the pedestal respectively. The term $H(w)$ represents the complex frequency response of the system, also known as Impulse Response or System Function or Transmissibility of the vibration isolator. In terms of physical parameters of the vibration isolator, the absolute transmissibility T is given by the equation :

$$T = |H(w)| = \left| \frac{X(w)}{U(w)} \right| = \sqrt{\frac{1 + (2R \frac{w}{w_0})^2}{[1 - (\frac{w}{w_0})^2]^2 + (2R \frac{w}{w_0})^2}} \quad (3)$$

where the undamped natural resonant frequency of the system w_0 is given by :

$$w_0 = \sqrt{\frac{K}{M}} \quad (4)$$

and the damping ratio R is expressed as :

$$R = \frac{C}{C_0} = \frac{C}{2\sqrt{KM}} \quad (5)$$

C_0 being the critical damping coefficient that equals $2\sqrt{KM}$.

Some Practical Considerations

The single degree of freedom system described above is an over simplified picture of an actual vibration isolator. Generally, the mass is supported on four springs and is split into parts (mass of platform, mounted equipment, etc.) so that the system has more than one degree of freedom and there is more than one resonant peak in the transmissibility versus frequency curve. In such cases, the system parameters (mass and damping) should be so chosen that the highest resonant frequency of the structure is considerably lower than the lowest frequency in the input spectrum to be isolated.

An important factor to be considered in multidegree of freedom systems is the lateral stability of the platform which often poses restriction on the softness of the spring to be chosen for fixing the platform.

Yet another factor in the above formulation is that the pedestal is assumed to be infinitely rigid. This assumption rules out any deformation with the application of external forces like, for example, those due to thermal changes. Under the effect of such deforming forces some more peaks are expected to occur in the transmissibility curve of the vibration isolator.

Thus, one can see that the transmissibility-frequency relationship of a vibration isolator is very complex, and that every peak in the corresponding curve needs to be examined carefully for an efficient isolator.

THE EXPERIMENTAL ARRANGEMENT USED

In order to measure the transmissibility of a vibration isolator, one needs to measure the amplitude spectra of ambient vibrations at the base (floor level), and on the top of the pedestal. The experimental set-up used is shown schematically in Fig. 2.

Two types of seismic sensors, namely a seismometer and an accelerometer were used to detect the ambient vibrations at the base and on the top of the pedestal. The seismometer is essentially a velocity transducer whose electrical output is proportional to particle velocity of ground motion. The operational sensitivity of this transducer is approximately 1.6 volts/cm/sec, and it has flat response in the frequency range of 1-100 Hz. The seismometer module can be arranged to detect either the horizontal or the vertical component of ground motion as required. The type of accelerometer used comprises a piezoelectric transducer whose electrical output is proportional to particle acceleration. Its sensitivity is close to 1 volt/g with flat response in a wide frequency band upto 800 Hz (PCB catalog G-500, 1990).

Electrical signals from all these sensors are preamplified (gain = 10) with the help of low-noise battery driven signal conditioners before recording on a four channel analog tape recorded in frequency modulation (FM) mode. For visual examination of waveforms, the tape replay is monitored on a two channel oscilloscope. For further analysis, we generated a number of seismic signals artificially by dropping a small weight on the floor near the sensors, by tapping the floor and suddenly starting and stopping a local vacuum pump.

PRELIMINARY ANALYSIS OF THE RECORDED SIGNALS

About three hours of tape recorded seismic signals obtained in different positions of the sensors and from various noise sources were replayed on a multi-channel ink jet strip chart recorder at a fast paper speed of 1000 mm/sec. The following preliminary results were obtained by visual examination of the traces :

- (1) The average ground displacement in vertical direction at the floor level is 72 nanometers (nm) predominantly in the frequency range of 30-35 Hz.
- (2) The average vertical ground displacement on the top of the pedestal is 30 nm in the same predominant frequency range of 30-35 Hz.
- (3) In both the horizontal directions (along the length as well as along the width of the pedestal), the average ground displacement on the top of the pedestal is nearly 2.5 times that at the floor level in the predominant frequency band of 30-40 Hz. These horizontal motions are estimated to be about 1.5 times the corresponding vertical displacement values mentioned at (1) and (2) above. This abnormal result may be attributed to some laterally driving forces that affect the structure in the following way. The top portion of the pedestal is disturbed additionally by direct air currents emanating from the cooling units installed albeit at sufficient height on the walls facing the length as well as the width of the pedestal. Although the sensors were kept covered for protection against such strong air currents reaching them directly, there was, unfortunately, no way to shut these cooling units of the central air-conditioning system to isolate the vibratory effects caused by them. Nevertheless, we have not considered for further analysis the horizontal vibration data contaminated possibly by the air currents.

SPECTRAL ANALYSIS OF AMBIENT VIBRATION DATA

About four seconds each of vertical component seismic noise records obtained on the floor as well as on top of the pedestal were hand digitised at a sampling rate of 500 samples/sec/channel and these data were subjected to detailed spectral analysis. Figures 3(a) and 3(b) show the amplitude spectra at the base and on the top of the pedestal respectively. If these two spectra are used to estimate the absolute transmissibility T of the pedestal, by just taking the ratio of the top and floor spectra ($X(w)/U(w)$) according to equation (2), the resulting function will be as shown in Fig. 3(c). There exist many spectral peaks in Fig. 3(c), which pose considerable difficulty in drawing definite conclusions regarding the actual transmissibility. Nevertheless, if one takes a look at the envelope of these amplitude spectra, one would notice that the floor level vibrations in the frequency band 20-50 Hz with maximum amplitude centred around 30 Hz does seem to be transmitted efficiently to the top of the pedestal, with little attenuation.

Since the pair of spectra in Figs. 3(a) and 3(b) comprise several peaks that essentially represent uncorrelated high frequency random noise, so does the spectral ratio in Fig. 3(c). These are none other than isolated spurious spectral peaks which can be suppressed (some of them can probably be eliminated) by generating a large number of the top and floor spectra and then taking their ensemble average.

Further Considerations Using Artificially Generated Signals

In the absence of an electronic analog to digital converter (machine digitisation), it is not only laborious but also cumbersome to handle manually a large number of noise records to produce sets of spectra required for deducing average picture

of transmissibility. On the other hand, we found it interesting and elegant to process and analyse data of artificially generated transient signals introduced at the time of the experiment. These transients were obtained by dropping a small weight on the floor at a distance of about 4 feet from the pedestal. The resulting records having small duration and reasonably large signal to noise ratio are easily handled. Moreover, they allow through coherence estimation more accurate determination of structural response compared to what one gets from ambient noise records as explained below (see, for example, John(1989), Crede & Harris(1976)).

Let us consider the vibration isolation pedestal as a kind of filter (Fig. 4) whose transfer function $H(f)$ (corresponding to $h(t)$ in time domain) is to be estimated. The output signal $x(t)$ of this filter is a composite of deterministic signal due to the input $u(t)$ and random uncorrelated noise $n(t)$, which is also the total noise present in the output. Thus,

$$x(t) = h(t).u(t) + n(t) \quad (6)$$

Taking Fourier transform of both the sides of equation (6),

$$S_x = H.S_u + S_n \quad (7)$$

where S_x , S_u and S_n denote the amplitude spectra of the output signal, the input signal and the total noise respectively. Multiplying both the sides of equation (7) with complex conjugate (S_u^*) of the input spectra,

$$S_x.S_u^* = H.S_u.S_u^* + S_n.S_u^* \quad (8)$$

or, simply,

$$S_{xu} = H.S_{uu} + S_{nu} \quad (9)$$

where S_{xu} is cross power spectra of the output and input signals, S_{uu} is input power spectra and S_{nu} is cross power spectra of the noise with the input signal.

After averaging, equation (9) becomes :

$$\overline{S_{xu}} = H.\overline{S_{uu}} + \overline{S_{nu}} \quad (10)$$

Assuming that S_n is small and that $\overline{S_{xu}}$ has been sufficiently smoothed by ensemble averaging which renders $\overline{S_{nu}}$ negligible, the cross power spectrum is simply given by :

$$\overline{S_{xu}} = H.\overline{S_{uu}} \quad (11)$$

Hence, the transfer function H reduces to :

$$H = \overline{S_{xu}} / \overline{S_{uu}} \quad (12)$$

To measure the degree to which the signal obtained on the top of the pedestal (output) is due actually to the signal on the floor level (input), we estimate coherence function γ which is expressed as follows :

$$\gamma^2 = \frac{[|\overline{S_{xu}}|]^2}{|\overline{S_{xx}}| |\overline{S_{uu}}|} \quad (13)$$

At a given frequency, the value of the coherence function gives the fraction of the output spectral power due to the input. For example, $\gamma = 1$ indicates a perfect spectral correlation between input and output signals, while $\gamma = 0$ refers to two completely different (independent) signals. The coherence helps to explain genuinity of some of the significant peaks in the response spectra.

RESULTS AND DISCUSSION

Based on the above method, typical transient signals generated by dropping a small weight on the floor are analysed and the transmissibility function is computed. Outputs from both the types of sensors, namely the seismometer and the accelerometer, are analysed separately in the frequency bands of DC-100 Hz and DC-300 Hz respectively. The upper frequency limit in the case of the seismometer recordings is imposed by the sensor response itself while that in the case of the accelerometer with relatively wider response is consistent with the chosen higher sampling rate of 1000 samples/sec.

Transmissibility from Seismometer Records

The waveforms of the artificially generated transient signals detected by the seismometers were sampled at the rate of 500 samples per second per channel upto a record length of 200 milliseconds (msec.). Figures 5(a) and 5(b) illustrate five such typical records (labeled 1 to 5) obtained at the base (input) and at the top of the pedestal (output) respectively. The input power spectra (floor level), the output power spectra (pedestal top) and the cross power spectra obtained by processing the basic signals prefiltered through a 100 Hz low-pass filter are shown in Figs. 6(a), 6(b) and 6(c) respectively. The point-to-point average of all the five traces in each set of Fig. 6 representing input, output and cross power spectra are shown in Figs. 7(a), 7(b) and 7(c) respectively. The computed values of coherence and transmissibility are plotted in Figs. 8(a) and 8(b) respectively. It is seen from Fig. 8 that the peak of the transmissibility curve occurs at 66 Hz and that at this frequency the coherence level is only 0.36.

However, these estimates are considered tentative and may not represent true transmissibility of the pedestal structure because the transmissibility maximum at 66 Hz is associated with low coherence at 36 percent (Fig. 8). This is due mainly to the band limited (DC-100 Hz) seismometer recordings which becomes evident in the following section where we analyse the accelerometer records having a relatively large bandwidth of DC-300 Hz.

Transmissibility from Accelerometer Records

The wide band (DC-300 Hz) transient signals from accelerometers were sampled at the rate of 1000 samples per second per channel. In Figs. 9(a) and 9(b) were reproduce for 100 msec duration typical records of four transient signals (labeled 1 to 4) detected by the accelerometer at the floor level and on the top of the pedestal respectively. Figs. 10(a), 10(b) and 10(c) show the corresponding input (floor level), output (pedestal top) and cross power spectra. The average of these sets of input, output and cross power spectra computed point to point as before are presented in Figs. 10(d), 10(e) and 10(f) respectively.

In this case, the average peak spectral power on the top of the pedestal (Fig. 10e) is found to be centred around 78 Hz followed by two relatively smaller peaks at 203 Hz and 258 Hz. On the other hand, the peak spectral power at

the floor level (Fig. 10d) is centred at 180 Hz in association with a smaller peak at 250 Hz and two still smaller peaks at 210 Hz and 86 Hz. The main features (peaks) of these three average power spectra (Figs. 10d-f) agree reasonably well with those of the constituent spectra (Figs. 10 a-c).

We shall now examine the estimates of wide band coherence and transmissibility which are plotted in Figs. 11(a) and 11(b) respectively. Corresponding to the five major and minor transmissibility peaks at 47 Hz, 78 Hz, 102 Hz, 195 Hz and 280 Hz seen in Fig. 11(b), the coherence function (Fig. 11a) has the largest value of 0.75 for the 102 Hz peak. The lowest coherence of 0.17 corresponds to the 78 Hz transmissibility peak and the intermediate (small) coherence values of 0.29, 0.27 and 0.25 correspond to the other three transmissibility peaks at 195 Hz, 280 Hz and 47 Hz respectively. The true transmissibility peak is thus established at 102 Hz. The other secondary maxima in the transmissibility curve are associated with very low coherence values (less than 50 percent of the maximum at 0.75). These are not significant and attributed mainly to the noise.

Considering that the band 90-110 Hz (Fig. 11b) containing the 102 Hz transmissibility peak has reasonably large coherence too (Fig. 11a), it is inferred that the transmissibility of the pedestal structure is appreciable in this particular frequency band. Outside this band the transmissibility diminished. The 66 Hz transmissibility peak (Fig. 8b) encountered during the analysis of the seismometric data does not seem to be pronounced as is evident from the accelerographic data (Fig. 11).

CONCLUSIONS

The transmissibility as a function of frequency of the typical concrete pedestal structure is computed in two different frequency bands : upto 100 Hz using seismometers and upto 300 Hz using wide band accelerometers. The true transmissibility is determined from the ratio of cross power spectra to the input power spectra of artificially generated transient seismic signals. The coherence function is also computed and is used as a tool interpret the transmissibility curve.

The pedestal is found to have appreciable transmissibility in the frequency band 90-110 Hz peaking at 102 Hz. The structure satisfactorily behaves as a vibration isolator in the higher frequency range beyond 110 Hz. In the lower frequency range below 90 Hz, however, some weak transmissibility does seem to exist implying that attenuation of vibrations in this frequency range is comparatively poor.

It would be interesting to examine if the high transmissibility around 102 Hz can be reduced by using softer materials like rubber or cork at the foundation. A small annular air gap of about 10 mm width separating the pedestal from the floor should indeed isolate some of the local floor vibrations more effectively.

ACKNOWLEDGEMENTS

This work was carried out as a follow-up of several intensive discussions between Dr. G. Krishnamurthy of Spectroscopy Division and Dr. S.K. Arora of Seismology Section, BARC, in an effort to achieve vibration free mounts for spectrometric systems. We thank Dr. V.B. Kartha of Spectroscopy Division, for his active participation in some of these discussions. We also thank Dr. F. Roy of Seismology Section for many useful discussions. Thanks are also due to Shri A.P. Mishra, Smt. Meenakshi and Smt. Saraswati P. of Spectroscopy Division

who rendered considerable assistance while taking experimental seismic measurements.

REFERENCES

1. Broch, J.T. (1972). Application of Bruel and Kjaer Instruments to Mechanical Vibrations and Shock Measurement, Bruel and Kjaer Application Note.
2. Crede, C.E. and C.M. Harris (1976), Shock and Vibration Handbook, Second Ed., McGraw Hill.
3. Hong Su, S. Rakheja and T.S. Shankar (1990), Vibration Isolation Characteristics of An Active Electromagnetic Force Generator and the Influence of Generator Dynamics, Trans. of ASME, J. of Vibration and Acoustics, Vol. 112, pp. 8-15.
4. Hunt, J.B. (1979), Dynamic Vibration Absorbers. Mech. Engg. Publ. Ltd., London.
5. John, D. (1989), Ambient Vibration Survey : Application, Theory and Analytical Techniques, Application Note No. 3, Kinematics, USA.
6. Krishnamurthy, G. (1991), Schematic Diagram of a Vibration Isolation Pedestal in Spectroscopy Division Laboratory, BARC, Personal Communication.
7. Lavania, B.V.K. and S. Bandyopadhyay (1989), Base Isolation for Foundation, Bull. Ind. Soc. Earthq. Tech., Vol. 26(4), pp. 1-14.
8. Newport Corporation (1989), About Vibration Control : Technical Product Catalogue of M/S Newport Corporation, USA.
9. PCB Piezotronics Inc. (1990), Seismic Accelerometer Model 393 C, Technical Catalog G-500, PCB Inc., USA.

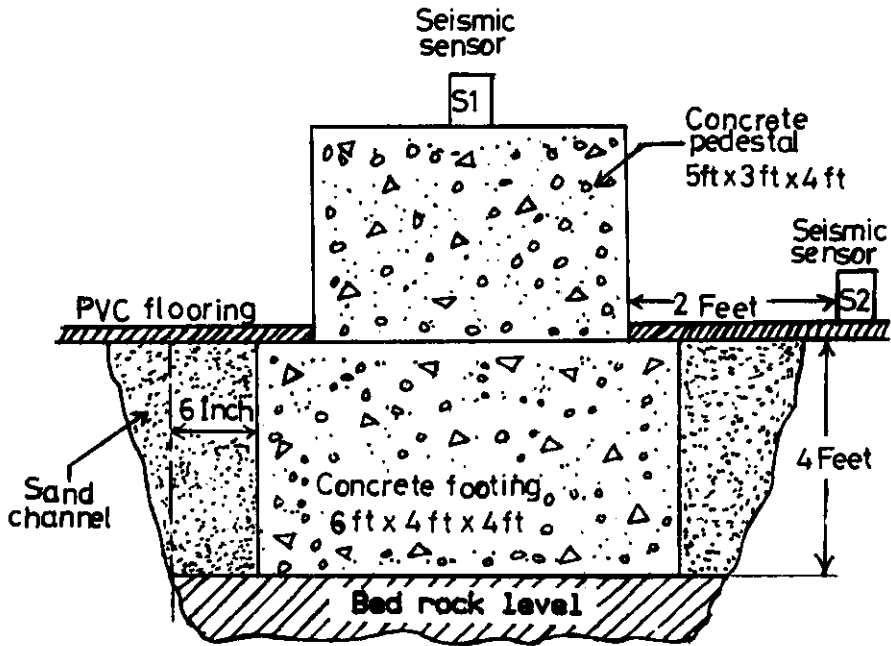


Fig.1 : Layout of typical concrete pedestal cast over bedrock.

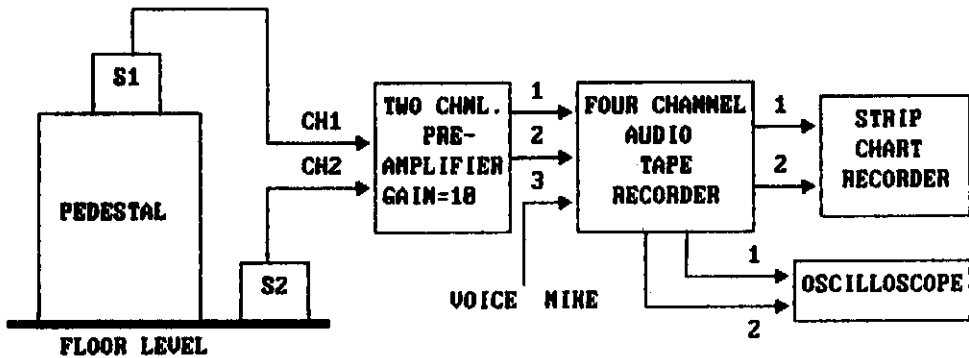


Fig.2 : Schematic block diagram of the experimental set-up used to measure the transmissibility of the concrete pedestal. S1 and S2 are seismic sensors (seismometers or accelerometers as the case may be).

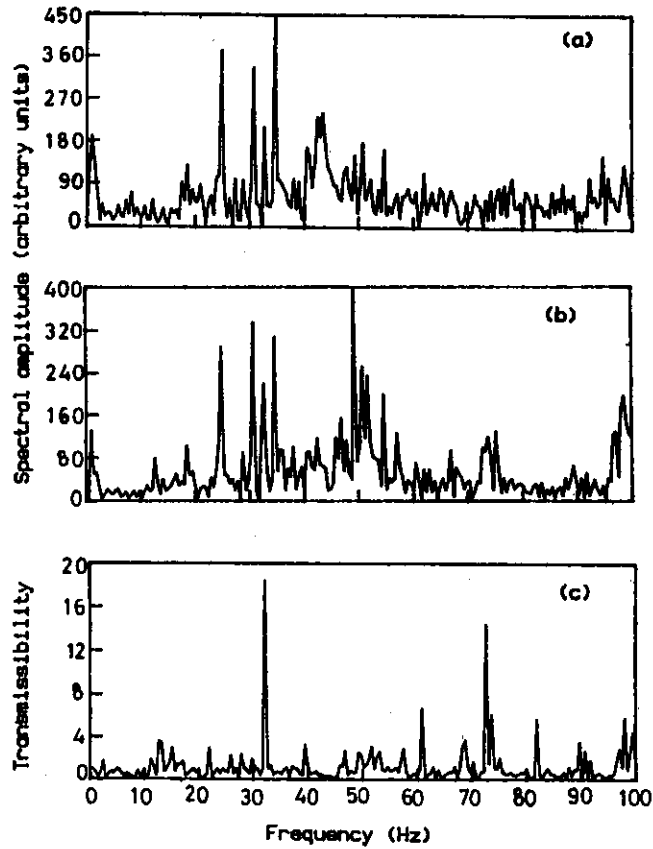


Fig.3 : Amplitude spectra of ambient seismic noise : (a) at the floorlevel (b) on the top of the pedestal. Transmissibility computed as the spectral ratio is shown in the bottom trace (c).

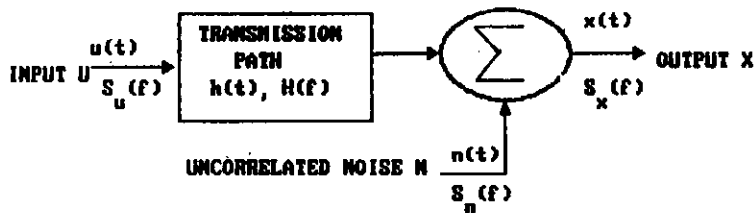


Fig.4 : Analytical model of the vibration isolation pedestal.

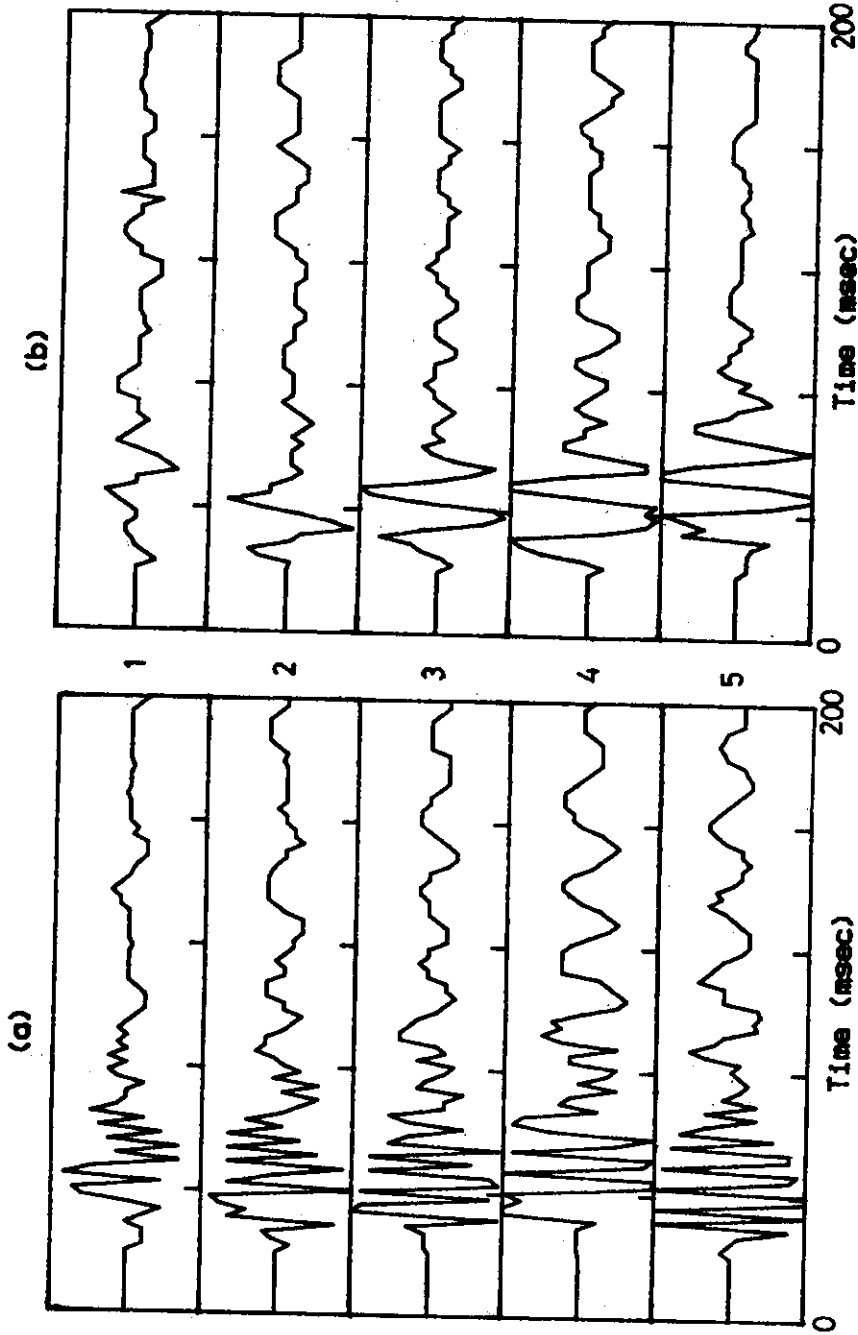


Fig.5 : Traces of five (labeled 1 to 5) typical transient signals detected by the seismometers: (a) at the floor level (input) and (b) on the top of the pedestal (output).

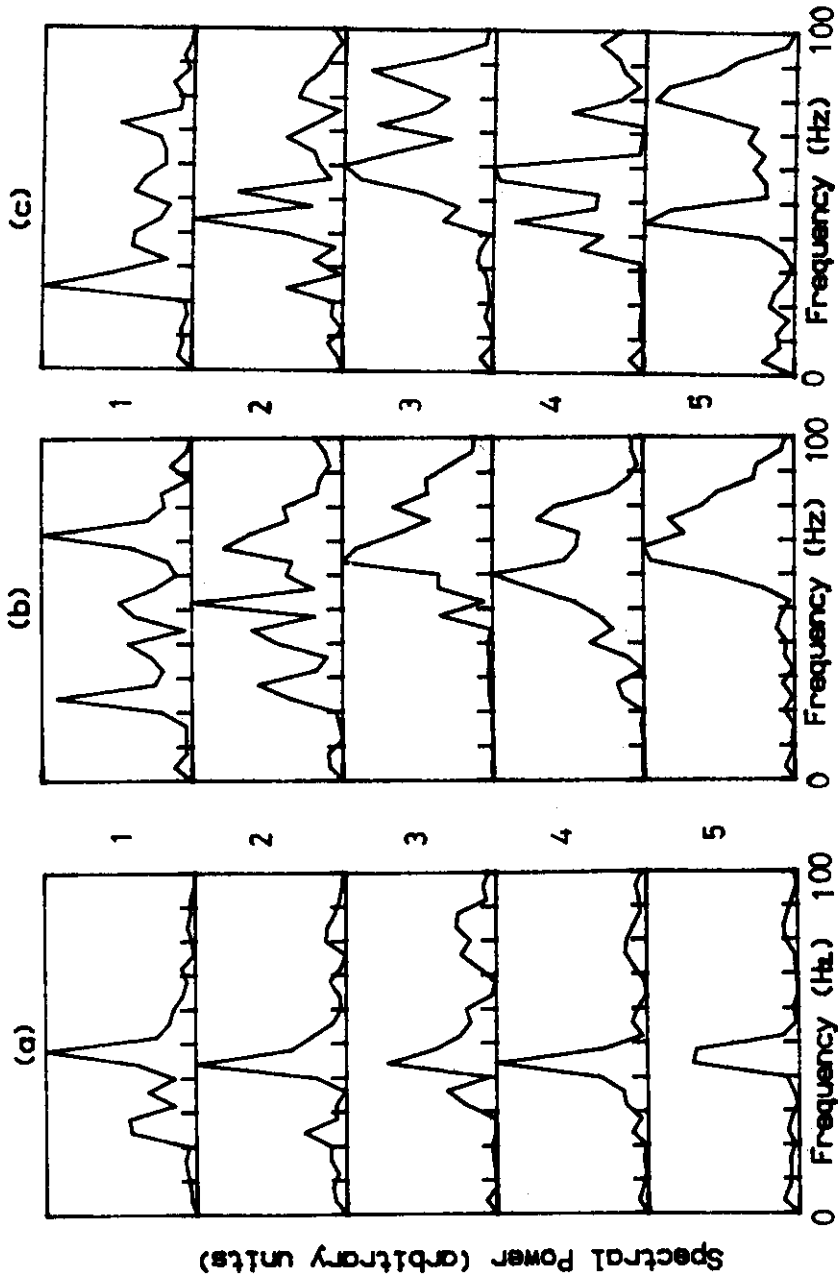


Fig.6 : Power spectra of prefiltered (DC-100 Hz) set of five typical transient signals depicted in Fig.5 representing (a) input (floor level vibrations), (b) output (top level vibrations) and (c) cross power spectra.

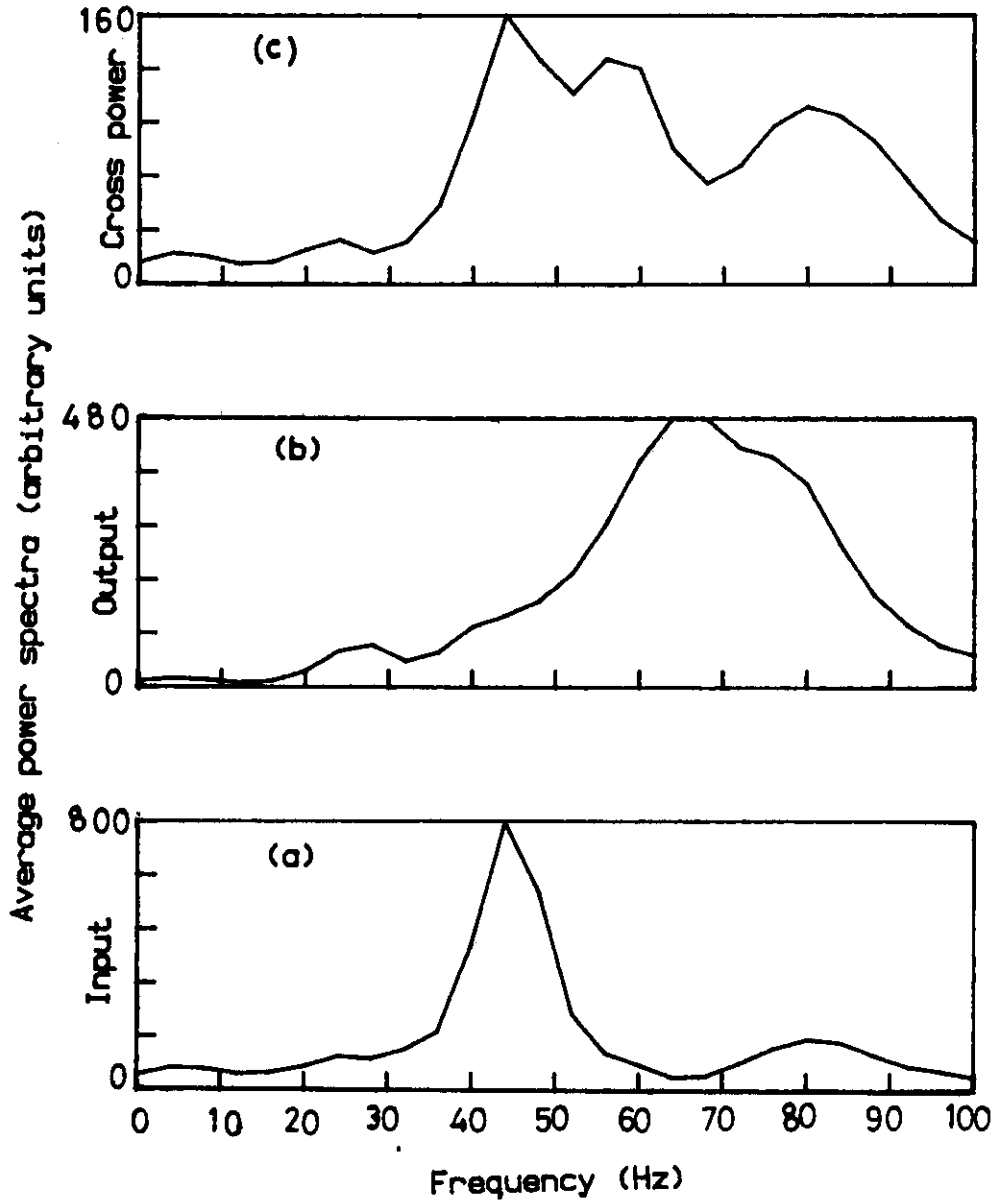


Fig.7 : Average of (a) input, (b) output and (c) cross power spectra depicted in Fig.8.

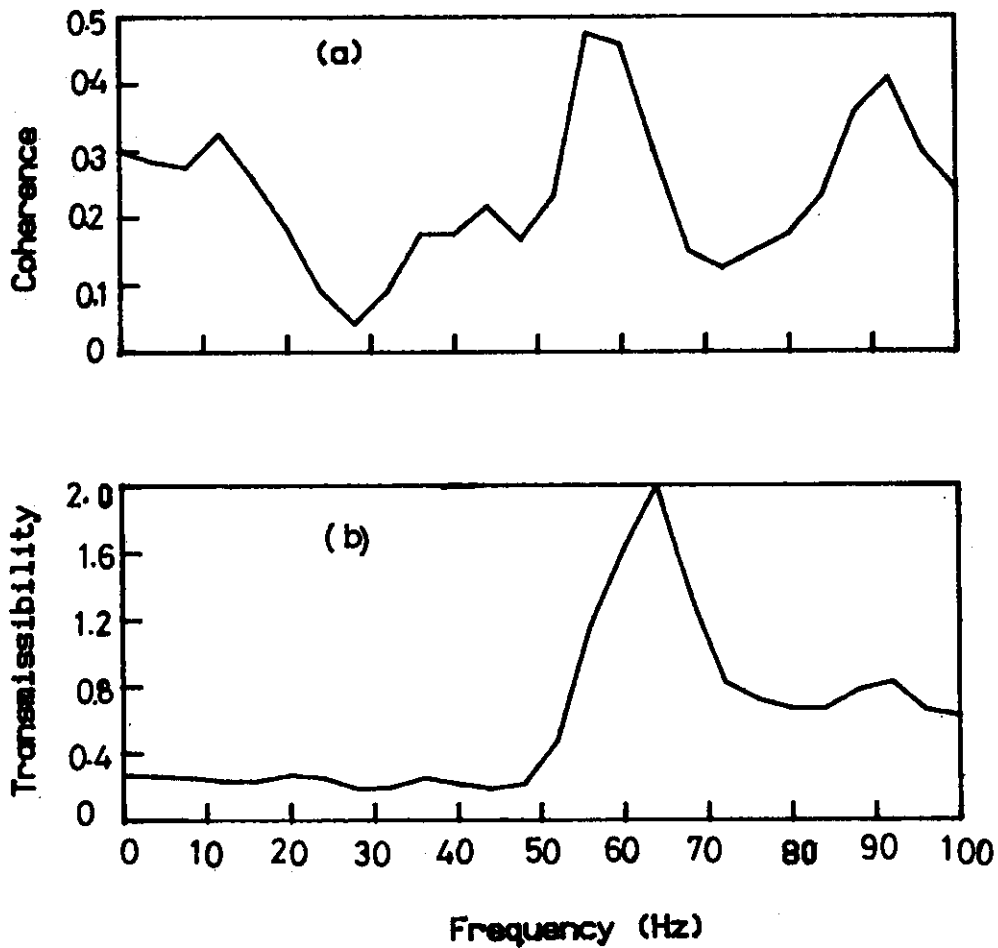


Fig.8 : Tentative estimates of (a) coherence and (b) transmissibility of the pedestal, based on band limited seismometer records.

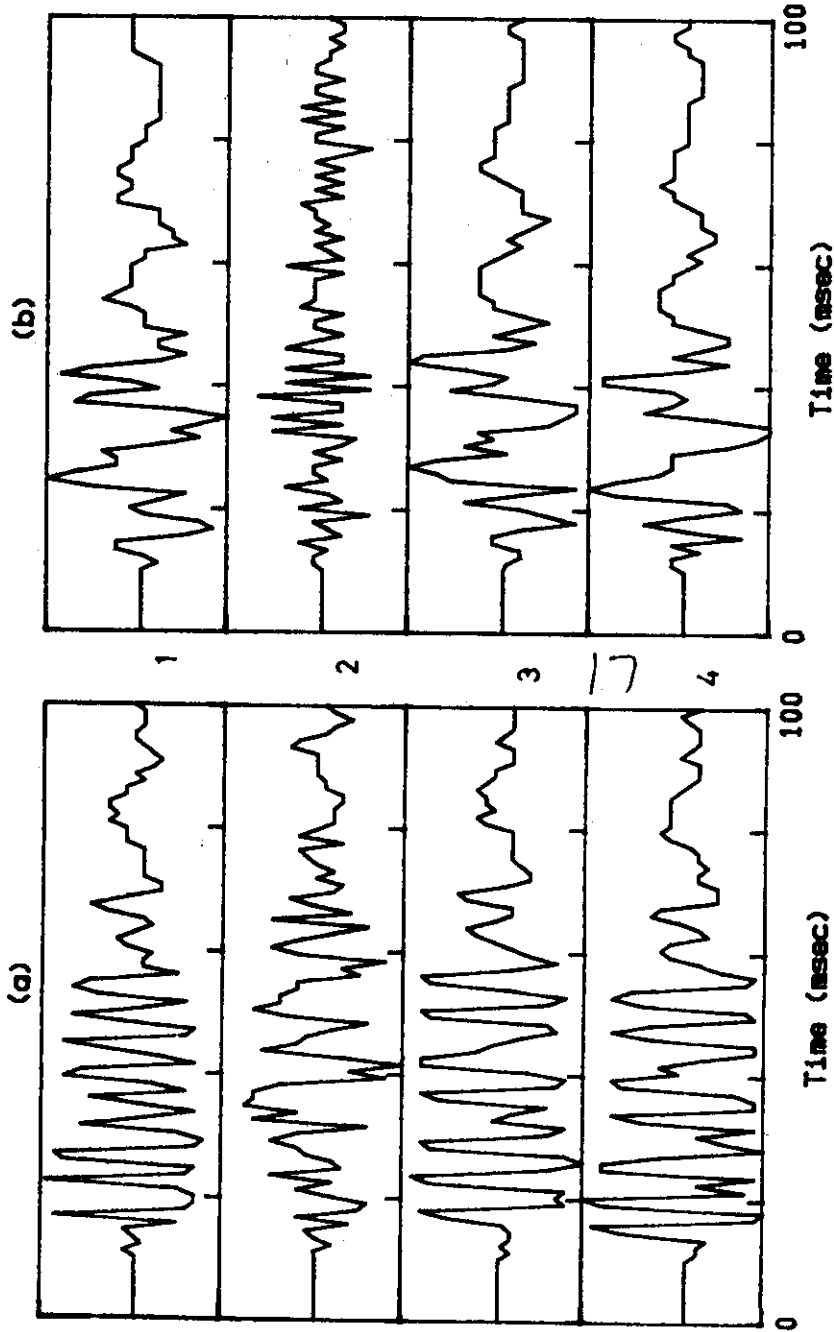


Fig.9 : Traces of four (labeled 1 to 4) typical transient detected by the accelerometers: (a) at the floor level (input) and (b) on the top of the pedestal (output).

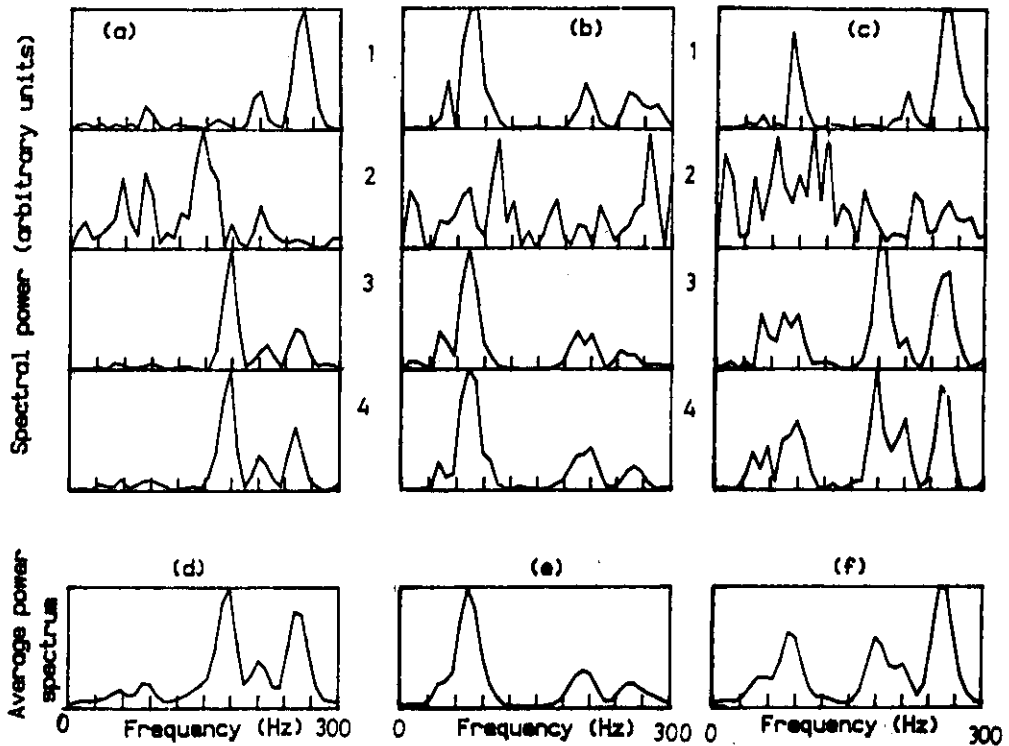


Fig.10 : (a) Input (floor level) power spectra, (b) output (pedestal top level) power spectra and (c) cross power spectra of the four signal traces depicted in Fig.9. The corresponding average spectra are shown in the insets (d), (e) and (f) at the lower end of the figure.

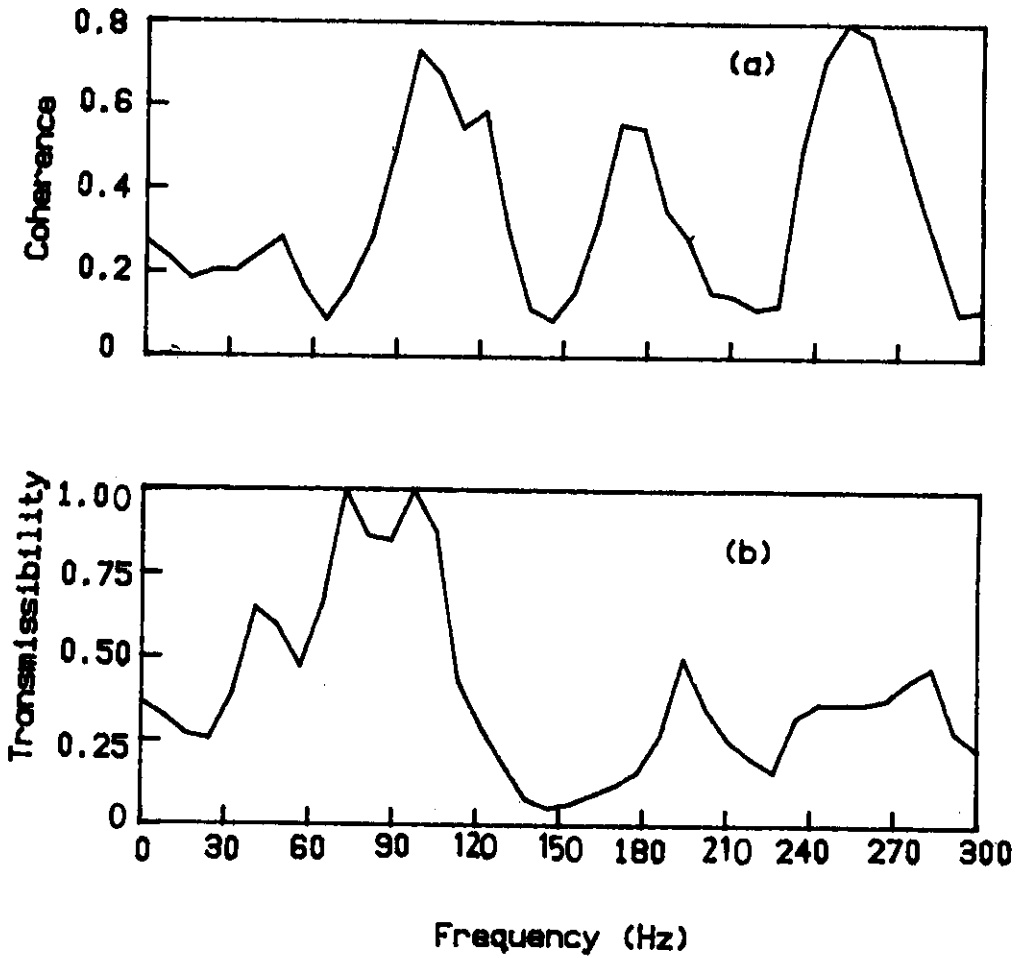


Fig. 11 : (a) Coherence and (b) true transmissibility of the pedestal, estimated from the wide band accelerometer records.